Numerical Modeling of Laser-Driven Turbulent Plasmas to Study Fluctuation Dynamo and the Role of Astrophysical Magnetic Fields

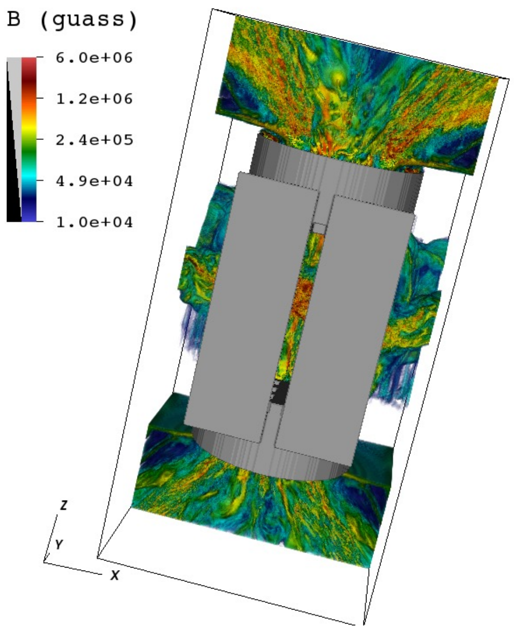

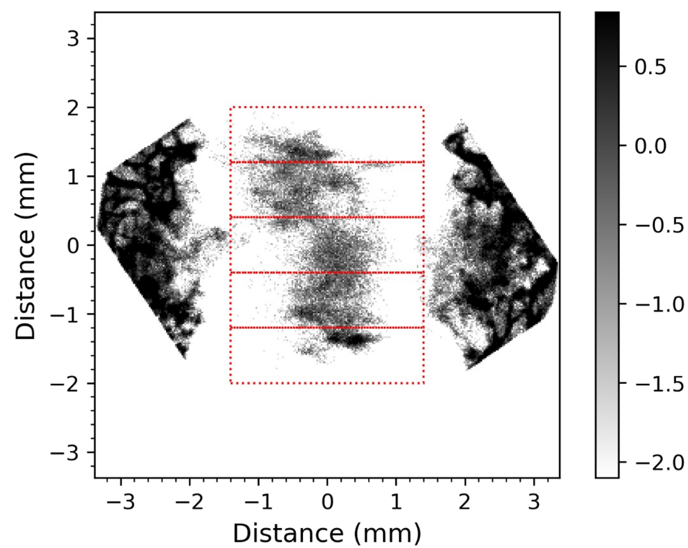

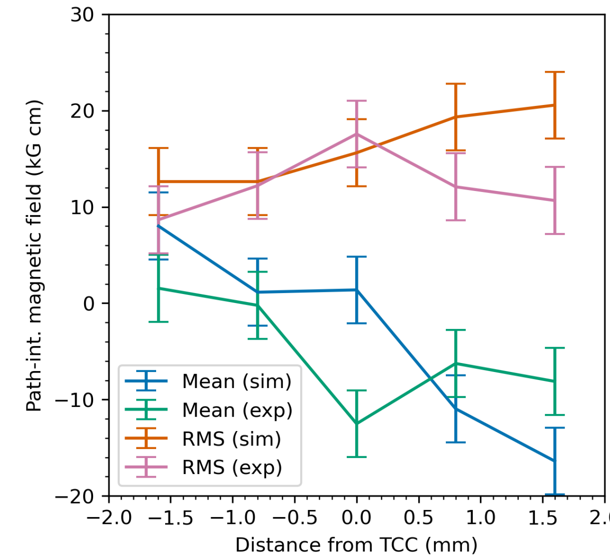

Yingchao Lu
Flash Center for Computational Science
Department of Physics and Astronomy
University of Rochester

64th Annual Meeting of the APS Division of Plasma Physics
October 17–21, 2022
Spokane, WA

TDYNO team collaborators

University of Rochester: A. Reyes, D. Froula, P. Tzeferacos
Princeton University: A. Bott
California State University Channel Islands: S. Feister
University of Oxford: J. Meinecke, H. Poole, L. E. Chen, A. A. Schekochihin, G. Gregori
Massachusetts Institute of Technology: C.-K. Li
Lawrence Livermore National Laboratory: H.-S. Park, B. A. Remington
Queen's University Belfast: C. A. Palmer
CEA France: A. Casner
University of Chicago: D. Q. Lamb

Thanks to our sponsors

- U.S. DOE NNSA under Awards DE-NA0002724, DE-NA0003605, DE-NA0003842, DE-NA0003934, DE-NA0003856
- NSF Award PHY-2033925
- Subcontracts 536203 and 630138 with LANL and B632670 with LLNL.

Summary

- We design the NIF experiment using FLASH simulations and create a turbulent plasma with magnetic field amplification under magnetic Reynolds number $\mathrm{Rm} > 10^3$ and magnetic Prandtl number $\mathrm{Pm} > 1$ condition, relevant to hot low-density plasmas found in astrophysical accretion disks and the intracluster medium (ICM).

- We study how fluctuation dynamo operates and amplifies magnetic fields under the conditions with suppressed electron thermal conduction, radiative cooling by high-Z elements and heating of the FABS probe beam.

- Proton radiography with partial obstacles reveal characteristics of the magnetic field distributions in the diffusive image.

- Two-color filtered X-ray self-emission images of the turbulent plasma reveal electron temperature distribution and the degree of thermal conduction suppression, relevant to the role of thermal conduction in active galactic nuclei (AGN) feedback.

- We study the role of thermal instability, relevant to thermal instabilities in galactic winds and haloes, and protostellar jets.

Magnetic fields and dynamo in the universe

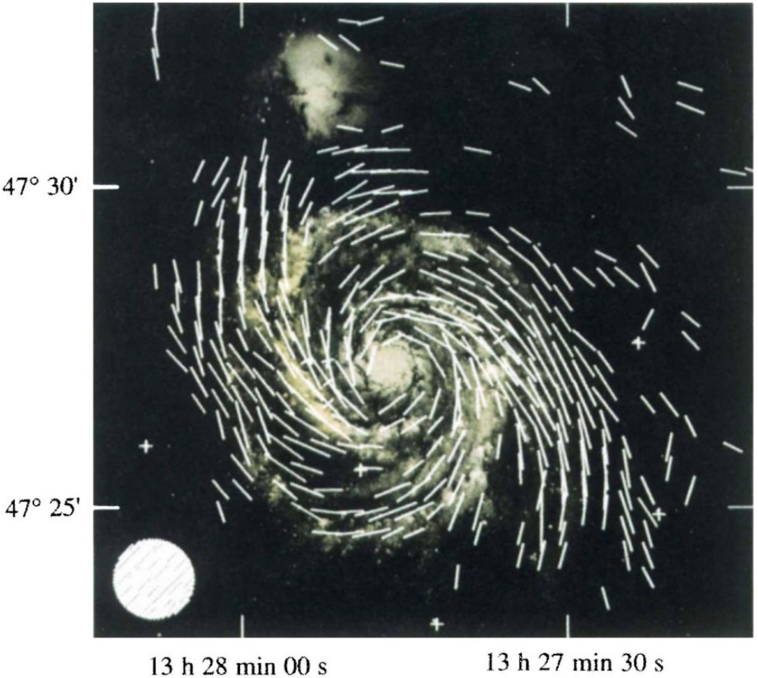

B-field vectors of M51 (Zweibel 1997)

$$\frac{\partial \mathbf{B}}{\partial t} + \mathbf{u} \cdot \nabla \mathbf{B} = \mathbf{B} \cdot \nabla \mathbf{u} + \eta \nabla^2 \mathbf{B} \qquad Rm \equiv \frac{\tau_{\mathrm{diff},\eta}}{\tau_{\mathrm{adv}}} = \frac{\mathcal{L}u}{\eta}$$

$$\frac{\partial \mathbf{u}}{\partial t} + \mathbf{u} \cdot \nabla \mathbf{u} = -\nabla P + \nu \nabla^2 \mathbf{u} + \mathbf{B} \cdot \nabla \mathbf{B} + \mathbf{f} \qquad Re \equiv \frac{\tau_{\mathrm{diff},\nu}}{\tau_{\mathrm{adv}}} = \frac{\mathcal{L}u}{\nu}$$

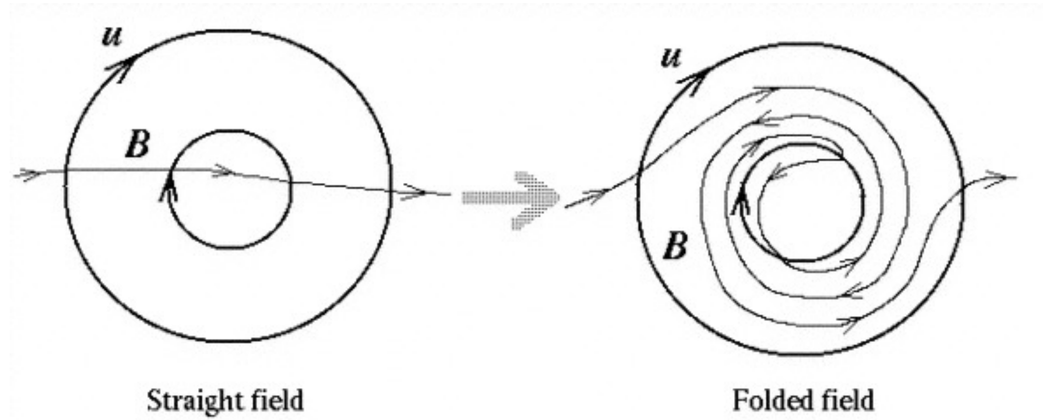

Stretching and folding of field lines by turbulent eddies (Schekochihin 2004)

- ❑ Seed magnetic field generation by Biermann battery effect (Biermann 1950) or Weibel instability (Weibel 1959)
- ❑ Dynamo amplified small-value seed fields to observed values (Parker 1979, Moffatt 1978, Kulsrud 1997)

Dynamo amplification experiments in Laboratory

Liquid Metal Dynamo Experiments

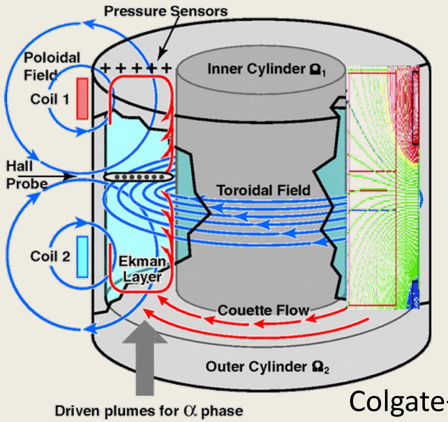

Colgate+ 2011

See also other liquid metal dynamo experiments:
Riga (Gailitis+ 2001)
VKS (Monchaux+ 2007)

Turbulent Dynamo at Omega Laser

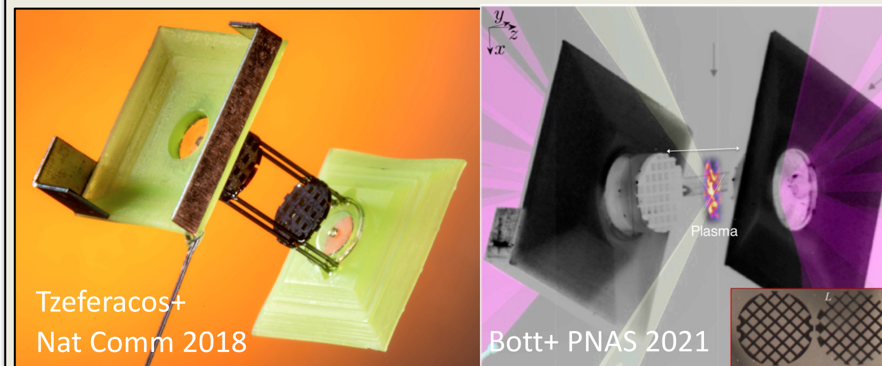

Rm ~ 600

Magnetic Field Amplification at Vulcan Laser

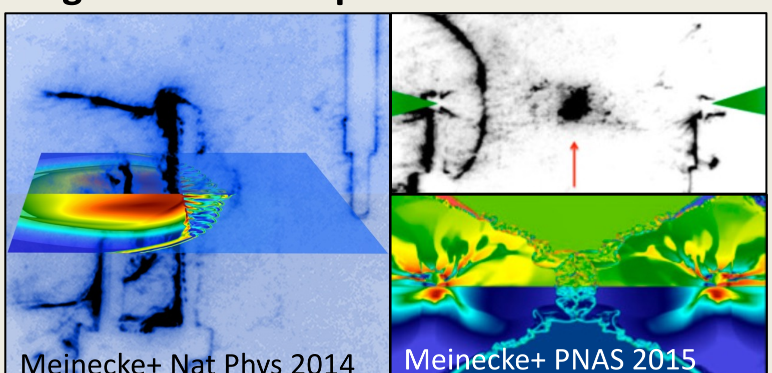

Rm ~ 3 - 6

NIF Dynamo Experiments and Effects on Heat Conduction

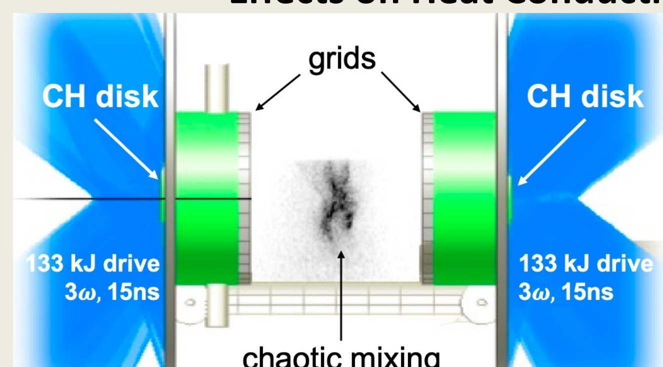

Rm ~ 3500

Meinecke+
Sci Adv 2022

The design of NIF laser-driven experiment to study fluctuation dynamo and the role of magnetic fields

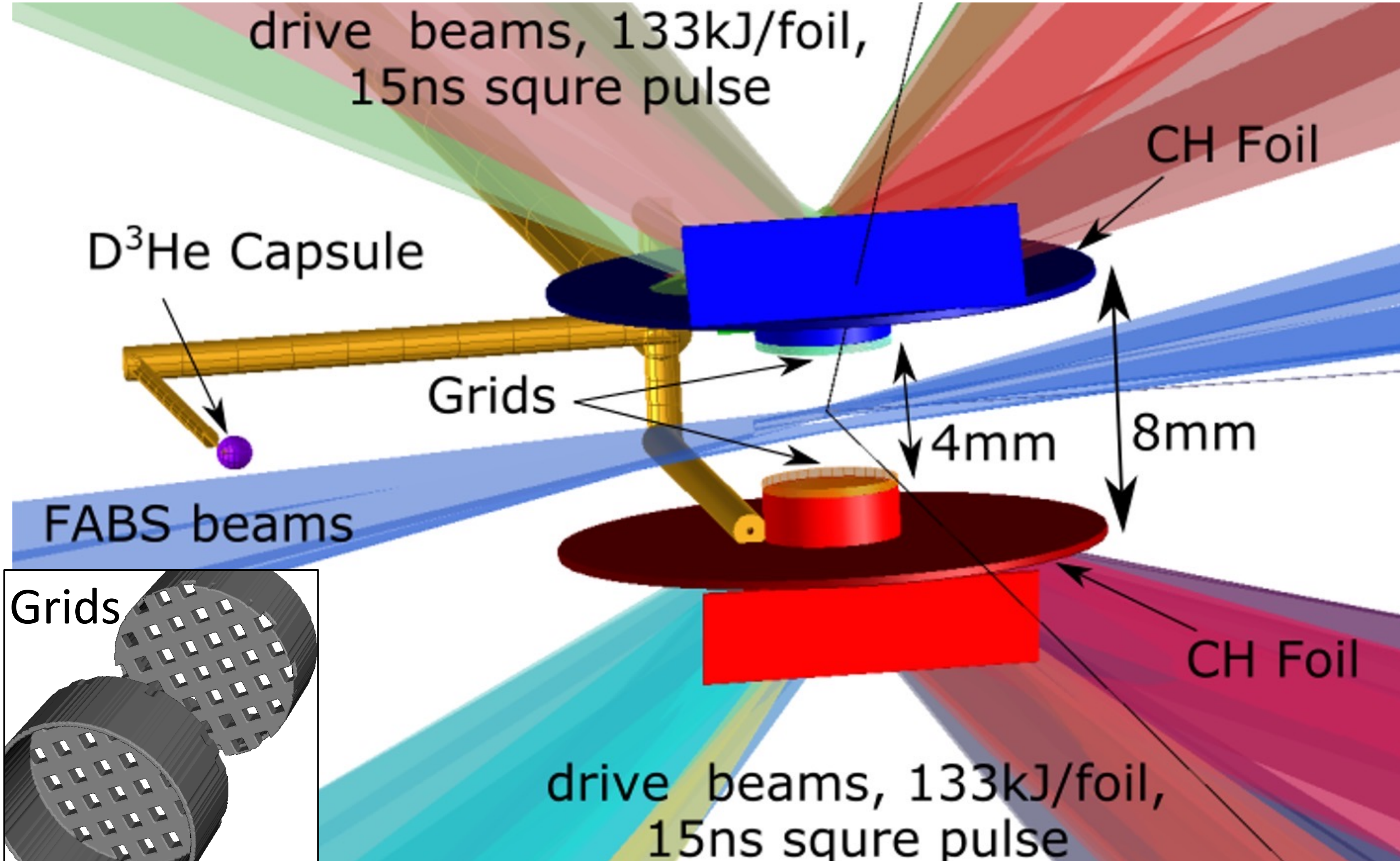

FLASH simulations predict interaction region condition for fluctuation dynamo to operate

Electron Number Density (cm^{-3})

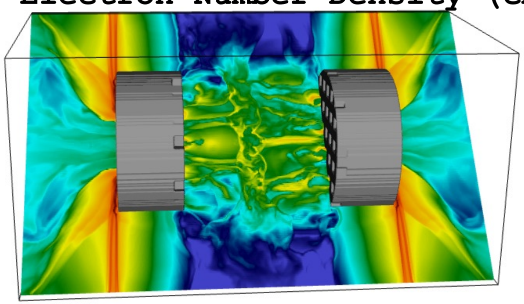

Electron Temperature (eV)

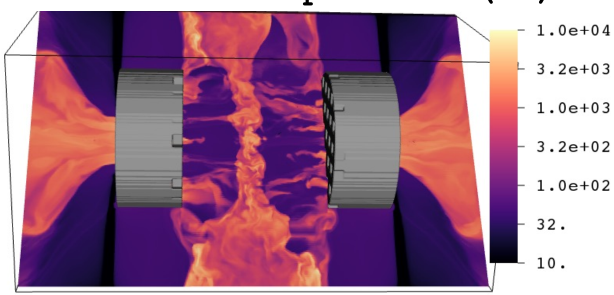

Magnetic Reynolds Number Rm

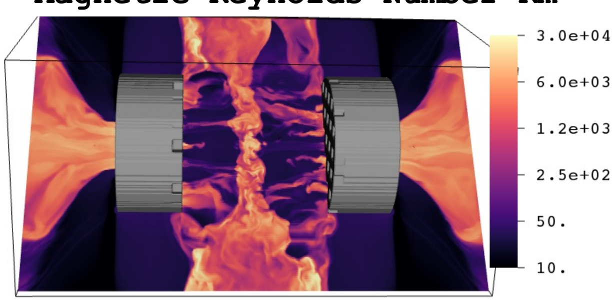

23 ns

Magnetic Prandtl Number Pm

$Pm = Rm/Re$

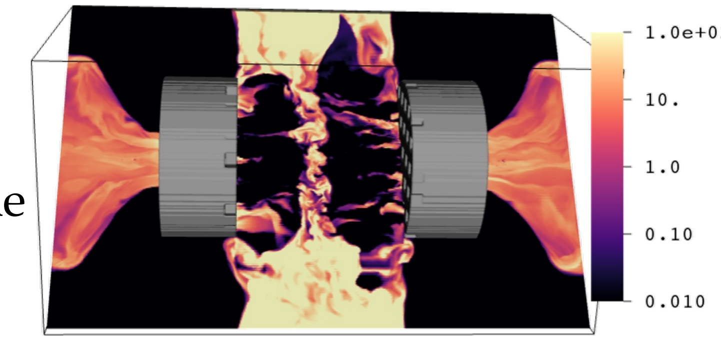

- The Interaction region turbulent plasma at 23 ns has reached the following condition:
  $u_{rms} \sim 2\times10^{7}$ cm/s,
  $n_e \sim 8\times10^{20}$ cm^{-3}, $T_e \sim 1300$ eV
  $Rm \sim 4.5\times10^{3}$, $Pm \sim 11$.
- The interaction region can locally have higher Rm and Pm.
- We reach the condition for fluctuation dynamo to amplify the seed magnetic field.

Dynamo amplification of the magnetic field

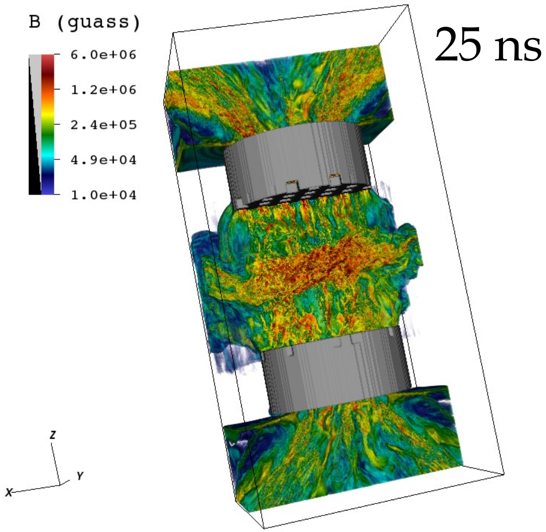

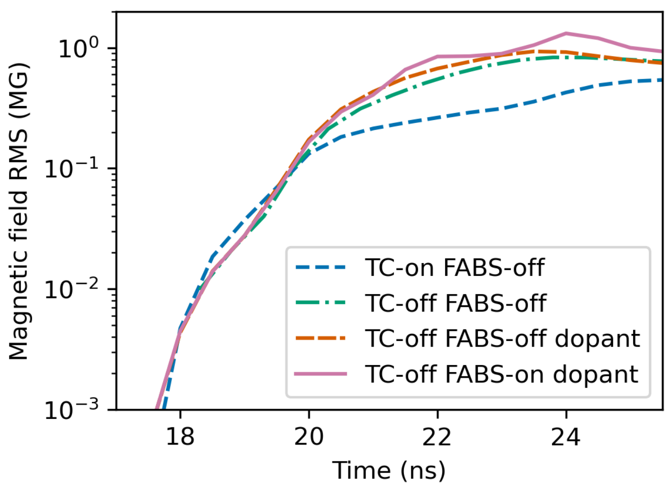

- ❑ As a result of the amplification, the magnetic field at 25 ns reaches a maximum value of ~4.7 MG and an RMS value of ~1 MG.
- ❑ The rise in the magnetic field at the central region is attributable to several factors: advection into the interaction region, compression, and turbulent dynamo.
- ❑ Suppression of electron thermal conduction (TC-off runs) and heating due to the FABS (full-aperture backscatter system) probe beams (FABS-on runs) result in an increase of the magnetic field strength.
- ❑ The plasma is self-consistently in the magnetized regime (i.e., the electron Larmor radius r_g < mean free path λ_e) with $r_g = 8.7\times10^{-5}$ cm and $\lambda_e = 1.1\times10^{-3}$ cm.

Proton radiography in the diffusive regime

25 ns

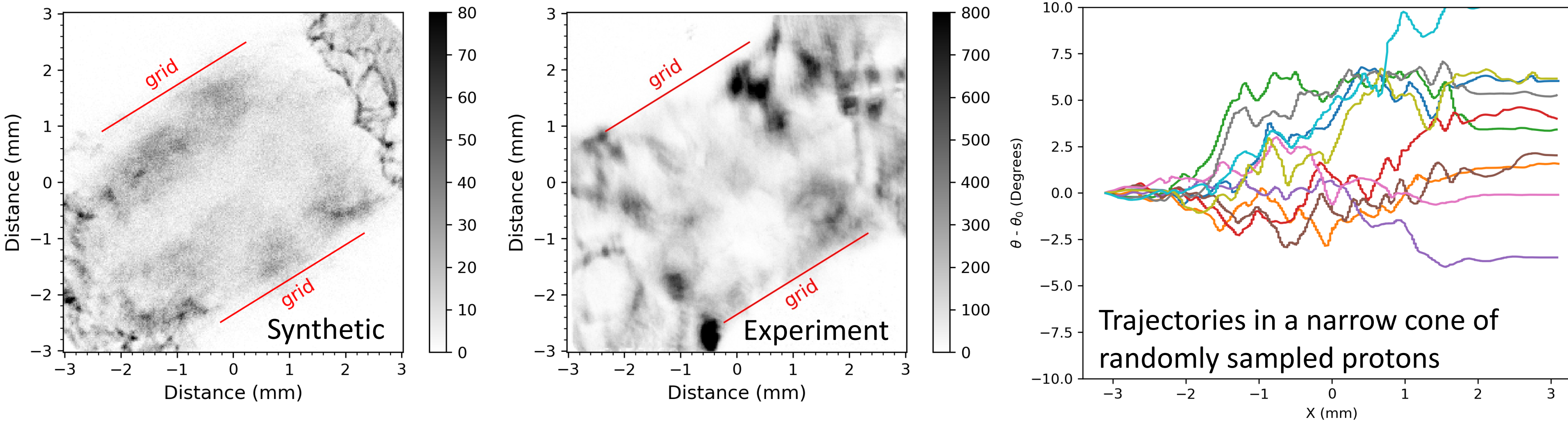

- Both the synthetic and experimental proton images are in the diffusive regime (Bott+ 2017) characterized as follows:
  - Synthetic proton trajectories from a narrow cone source have crossings before they leave the plasma.
  - The correlation length of the magnetic field is $l_B = 0.0045$ cm, which is less than the RMS perpendicular displacement of protons going through the interaction regime plasma due to magnetic deflections $l_z\delta\theta=0.03$ cm.

Proton radiography with slit shield provide measurements of axial magnetic fields

25 ns

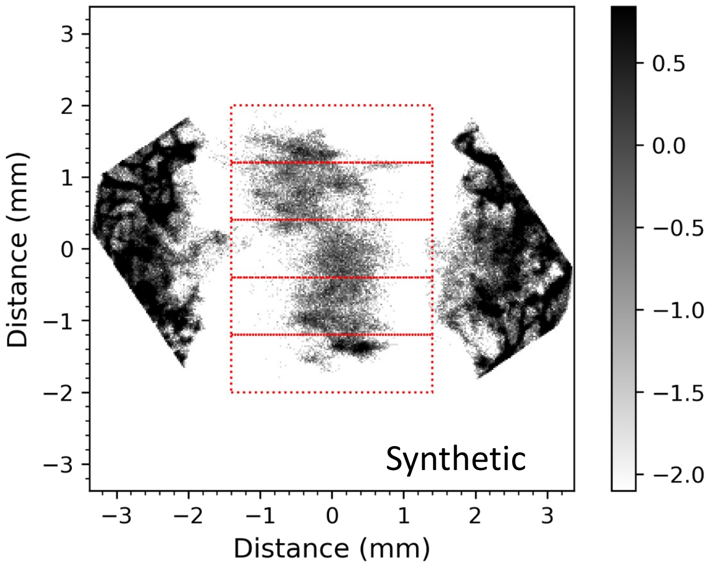

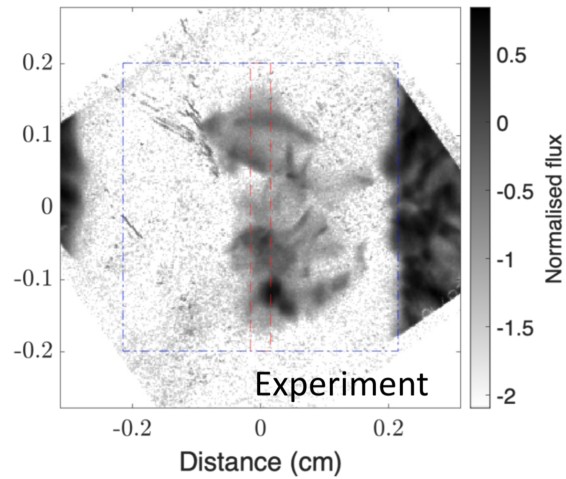

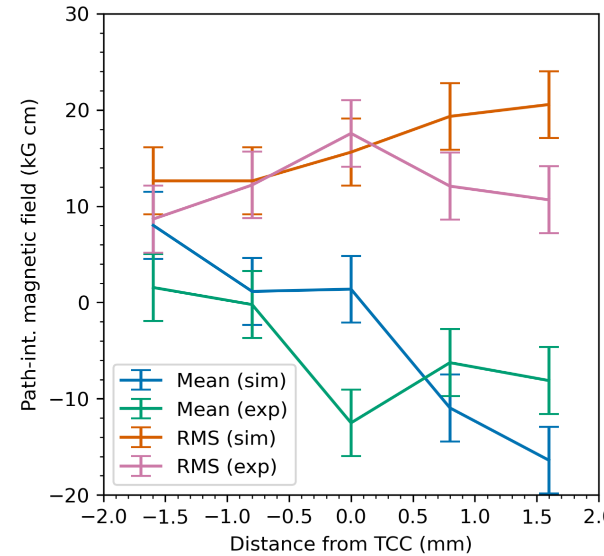

- There are a significant number of protons deflected from the unshielded regions by strong magnetic fields.
- Using a slit shield, we measured the axial magnetic field in synthetic proton images and experimental data. (method developed in Bott+ 2017 and used in Chen+ 2020)
- The trend and magnitude of the magnetic field in the experimental data is comparable to the one inferred from the synthetic image.

Factors affecting electron temperature and density

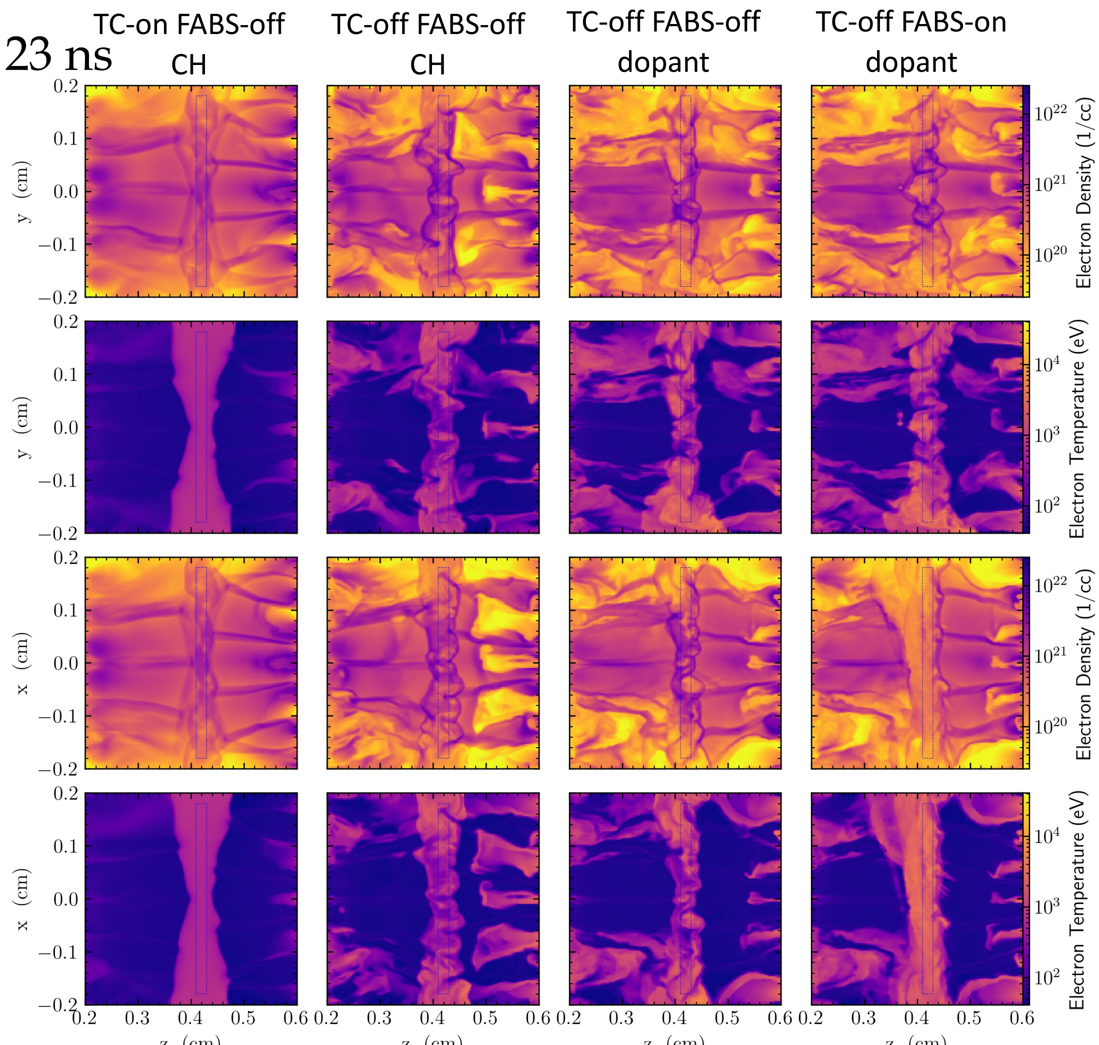

- By turning the thermal conduction off before the interaction region forms, the electron temperature distribution has more small-scale structures due to thermal instability (cooling instability).
- In dopant runs, cooling instability plays a more important role.
- FABS heating increases the temperature only where the FABS beams intersect the interaction region.

Temperature distribution affected by conduction-off, FABS, and dopants

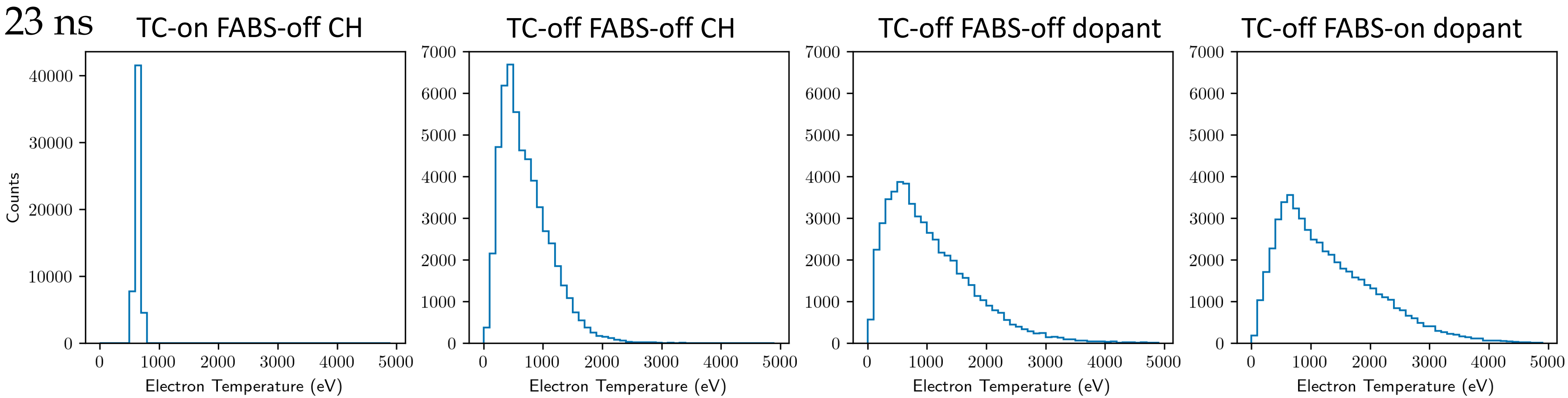

- By turning the thermal conduction off (TC-off), the electron temperature is broader, and the thermal instability is already in the nonlinear stage.
- The dopant run has a prominent tail in the electron temperature distribution due to stronger thermal instability.
- FABS heating does not significantly affect the overall electron temperature distribution.

Pressure equilibrium and thermal instability growth rate

23 ns

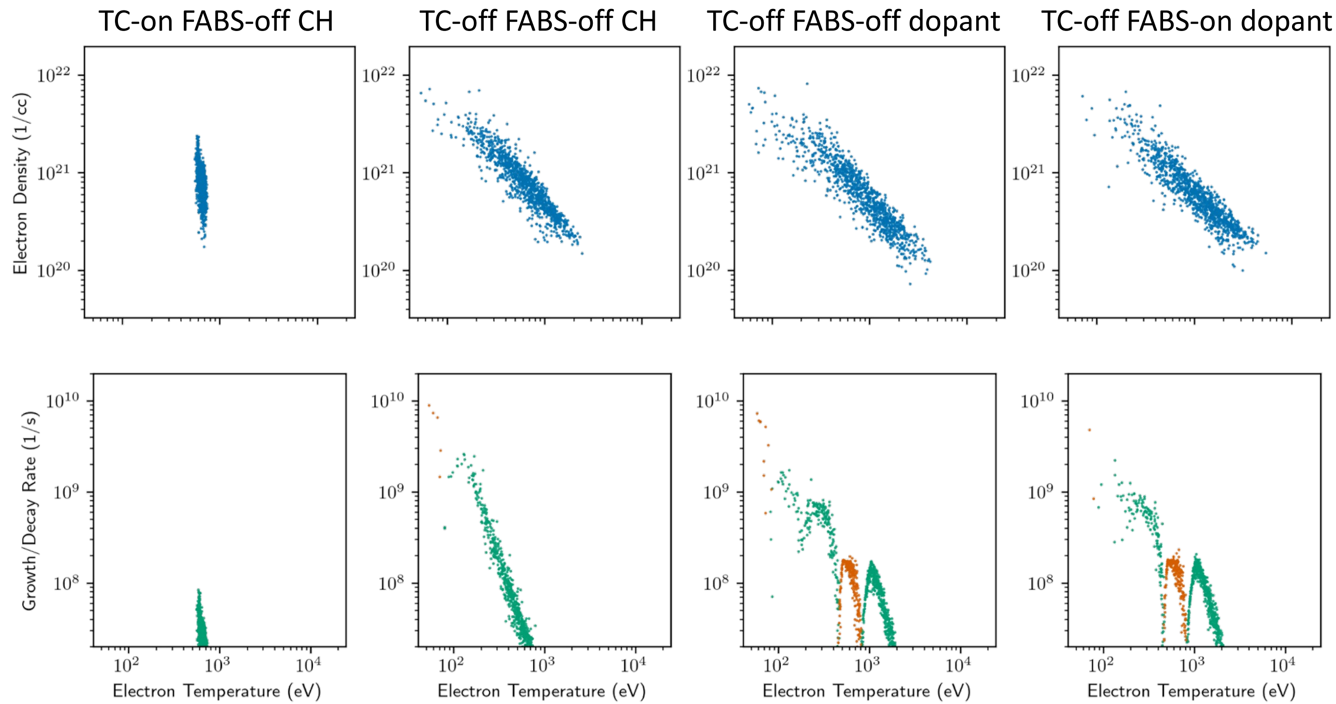

- In TC-off runs, pressure is in equilibrium, which is consistent with the fact that the <u>sound wave mode</u> growth rate $\Gamma_{Cs} << 1/\tau_{exp} = 4.0\times10^{7}\,s^{-1}$. (calculated from PROPACEOS table using growth rate in Field 1965 and Hunter 1970)
- The growth rate of the <u>collapse mode</u> is larger for dopant runs (shown in the second-row figures), i.e., $\Gamma_{Collapse} \sim 1/\tau_{exp}$.

Inferring electron temperature distribution from synthetic X-ray self-emission images

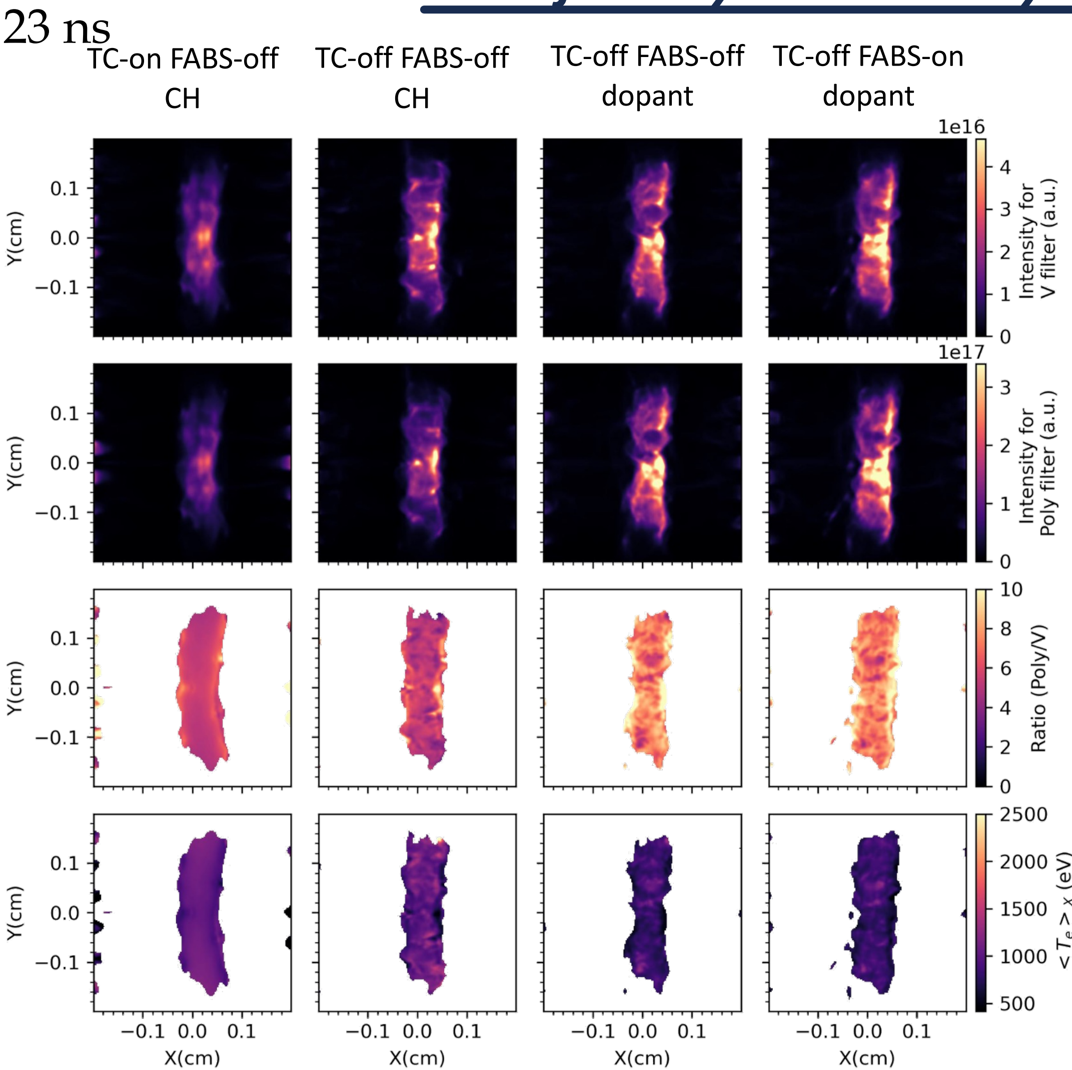

- ❑ The highly structured electron temperature profile in the TC-off runs results in highly structured X-ray self-emission intensity.
- ❑ The ratio of intensity filtered by V and polyimide is related to the line-of-sight mass-averaged temperature.
- ❑ The suppression of electron thermal conduction has been demonstrated in the experiment (Meinecke+ Sci. Adv. 2022, previous talk by Archie Bott14).

Summary

- We design the NIF experiment using FLASH simulations and create a turbulent plasma with magnetic field amplification under magnetic Reynolds number $\mathrm{Rm} > 10^3$ and magnetic Prandtl number $\mathrm{Pm} > 1$ condition, relevant to hot low-density plasmas found in astrophysical accretion disks and the intracluster medium (ICM).

- We study how fluctuation dynamo operates and amplifies magnetic fields under the conditions with suppressed electron thermal conduction, radiative cooling by high-Z elements and heating of the FABS probe beam.

- Proton radiography with partial obstacles reveal characteristics of the magnetic field distributions in the diffusive image.

- Two-color filtered X-ray self-emission images of the turbulent plasma reveal electron temperature distribution and the degree of thermal conduction suppression, relevant to the role of thermal conduction in active galactic nuclei (AGN) feedback.

- We study the role of thermal instability, relevant to thermal instabilities in galactic winds and haloes, and protostellar jets.